© Universiti Tun Hussein Onn Malaysia Publisher's Office

**IJIE**

http://penerbit.uthm.edu.my/ojs/index.php/ijie
ISSN : 2229-838X e-ISSN : 2600-7916

The International Journal of Integrated Engineering

# Development of Nonlinear Adaptive PI Controller For Improved Pneumatic Actuator System

**S. I Samsudin[1*], Siti Fatimah Sulaiman[1], Khairuddin Osman[1], S. I. M. Salim[1], Sazuan Nazrah Mohd Azam[2]**

[1]Faculty of Electronics and Computer Engineering,
Universiti Teknikal Malaysia Melaka, Hang Tuah Jaya, Durian Tunggal, Melaka, 76100, MALAYSIA

[2]Faculty of Electrical Engineering,
Universiti Teknikal Malaysia Melaka, Hang Tuah Jaya, Durian Tunggal, Melaka, 76100, MALAYSIA

*Corresponding Author

DOI: https://doi.org/10.30880/ijie.2022.14.06.018
Received 06 September 2021; Accepted 14 June 2022; Available online 10 November 2022

**Abstract:** The wide application of pneumatic actuator in electrical and electronics sectors are undeniable hence ask for a good control environment. PID controller is always known with easy implementation and good control performance. But the limitation of the PID static gains to effectively control the complex nonlinear system is unavoidable. This suggests the enhancement of the PI controller with a nonlinear adaptive interaction algorithm (AIA) thus develop the nonlinear adaptive AIA PI. The modification is introduced by integrating a nonlinear gain function that adaptively tunes the AIA parameter, hence resulting the best tuning of the PI control gains. The nonlinearities inherent in the system parameters are believed to be handled by the integration, therefore improving the controller performances while maintaining the pneumatic actuator at the desired position. It was proved that improved error performance criteria's, settling time and overshoot were resulted by the nonlinear adaptive AIA PI compared to fix adaptive AIA PI, and significantly good compared to conventional PID and PI controllers. Besides, about 19.72%, 11.72%, and 0.22% overshoot were successfully reduced by the nonlinear adaptive AIA PI compared to optimal PSO PI, PSO PID, and PSO AIA, respectively. To conclude, the development of the proposed controller is demonstrated to function well and offers an alternative tuning strategy in other electrical and electronic engineering applications.

**Keywords:** Pneumatic actuator control, adaptive PI, adaptive interaction algorithm (AIA), nonlinear adaptive PID, nonlinear gain function

## 1. Introduction

The pneumatic actuator system is widely applied in industrial automation of electrical and electronics sectors due to its high-power ratio, cleanliness of fluid medium, and lower-cost devices. However, difficulties come to accomplish a good position control of pneumatic actuator caused by the complex nonlinearities and uncertainties issues such discussed in [1-2]. There are many works focused to enhance the performance of a pneumatic actuator. The study applies an intelligent pneumatic actuator (IPA) system that integrates actuator, sensors and microprocessor in the system. Compared to other conventional pneumatic actuator, the IPA system is more complicated in which constantly deals with the valve dead zone, air leakage, air compressibility, and friction in the system's parameters hence ask for a more complicated control process [3-6].

**Corresponding author: author@organization.edu.co*

In fact, a proportional-integral-derivative (PID) controller is a broadly employed control strategy due to its easy implementation and good control performance. In order to minimize the error, the PID deals with the proportional gain, *Kp*, integral gain, *Ki*, and derivative gain, *Kd*. However, the conventional PID comes with the fixed or static gains, challenging to perform well against the time-variant system. Therefore, the enhancement of the PID with self-tuning technique and/or combination with artificial algorithm and/or optimal algorithm are widely studied in many research works such reviewed in [1]. An adaptive Fuzzy PID and a cascade Fuzzy self-adaptive PID were successfully applied to electro-pneumatic system and to the pneumatic actuator position in [7] and [2], respectively. A fuzzy-based fractional-order PID (FFOPID) controller has been applied in [8] for a robust performance with respect to load variation and external disturbances of a pneumatic pressure system. The effectiveness of the FFOPID has been proved by improved settling time, percentage overshoot, ISE and, IAE resulted compared to conventional PID. Further, the enhancement of the PID with the nonlinear gain function and the PSO optimization algorithm for optimal pneumatic positioning control was superiorly implemented in [9-10]. These studies show good control performances, but high experiences on the practical system and complicated tuning processes were always demanded.

The development of the IPA system and the first application of the proportional-integral (PI) controller to the IPA were detail explained in [11-12]. It then continued by the implementation of the pole-placement feedback controller and PI with bang-bang controller as discussed in [13] and [14], respectively. The study to control the IPA system was extended to predictive functional control (PFC) and model predictive control (MPC), such presented in [3-5, 15]. Even though both the PFC and MPC offer good tracking potential and overshoot, but it highly asks for a complex control strategy.

The study aims to develop a simple but effective control algorithm for a pneumatic actuator system. This motivates the development of a adaptive PI controller based on an adaptive interaction algorithm (AIA). The AIA has been introduced in [16-17]; it is one of the direct adaptation methods for online tuning tasks that have the potential to update the control parameters without explicit estimation of the plant model parameters. The AIA was demonstrated to adapt and control different natures and types of the system, including linear and nonlinear systems, and can be used in time-variant systems besides being easy in derivation and implementation. The Lyapunov stability theory explains the stability of the algorithm in [17]. A simple and effective way of performing the gradient descent in the parameter space was also explored. A self-tuning PID based on AIA controller has been designed in tracing the command signal for the pitch, roll, and yaw of a quadrotor unmanned aerial vehicle (UAV) system in [18]. Meanwhile, [19] successfully applied adaptive AIA PID for a three-phase brushless DC motor drive framework while [20] proves improved control performance of the wastewater treatment plant using the AIA. Besides, the algorithm was also patterned in reducing the combustion engine crankshaft speed pulsation as presented in [21].

According to AIA, the PI control system is divided into three subsystems: the proportional control part, the integral control part, and the pneumatic control part while the *Kp* and *Ki* parameters of the PI being the interactions between these subsystems. With the self-tuning algorithm, the controlled system keeps updating its response due to changes of the input with respect to time to achieve good output responses. But difficulties come to identify the best value for the unknown fix AIA parameter especially when deals with complex nonlinear systems. This leads the new modification of the adaptive AIA PI to be integrated with a nonlinear gain function applied in [22], hence developing the nonlinear adaptive AIA PI controller. It is believed that the parameter of the nonlinear AIA results the best tuning of *Kp* and *Ki* control gains therefore superiorly improve the transient response of the pneumatic actuator positioning.

The paper is divided into 4 sections. Section 1 discusses the introduction and the background of the proposed work. The brief on the pneumatic actuator system, continued by the PI controller, the theoretical concept of the adaptive interaction algorithm, and the proposed controller's development, are next explained in Section 2. Section 3 presents the result and discussion of the controller, while the conclusion of the paper is explained in Section 4.

## 2. Methodology

### 2.1 Intelligent Pneumatic Actuator System

Figure 1 shows the system architecture of the intelligent pneumatic actuator (IPA). The IPA system is equipped with a programmable system on chip (PSoC) circuit board, two valves, optical and pressure sensor, and a laser stripe rod. KOGANEI-ZMAIR optical sensor is used where smaller pitch of 0.01 mm can be detected. The sensor is mounted on the top of the cylinder to detect the position of the cylinder stroke based on the position reading given by the laser stripe rod. Besides, there are on/off valves attached toward the end of the cylinder to monitor and control the inlet and outlet air of the cylinder. A programmable system on chip (PSoC) board was integrated into the cylinder that function to control the pneumatic system's whole operation. There are two chambers applied where the chamber 1 is fixed at constantly 0.6 MPa pressurized air while the control action highlights at only one chamber (chamber 2). Therefore, the extension and retraction of the cylinder stroke are due to the duty cycle of a pulse-width modulator (PWM) signal to drive the valves on the chamber 2. This makes the referred pneumatic system different from other available pneumatic actuators, hence contributing to the research work's uniqueness. The detail development of the IPA system can be referred in [6].

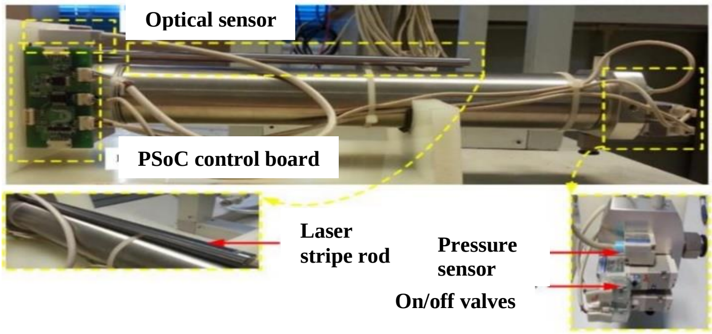


**Fig. 1 - The pneumatic actuator system**

A system identification technique in Matlab System Identification Toolbox is applied to represent the dynamic behavior of the IPA system. Figure 2 illustrates the process used to obtain the input and output data based on an experimental approach that consists of National Instrument (NI) DAQ card PCI/PXI-6221 (68-Pin) board, which linked to the PC, and SCB-68 M series devices with a SHC68-68-EPM cable connector.

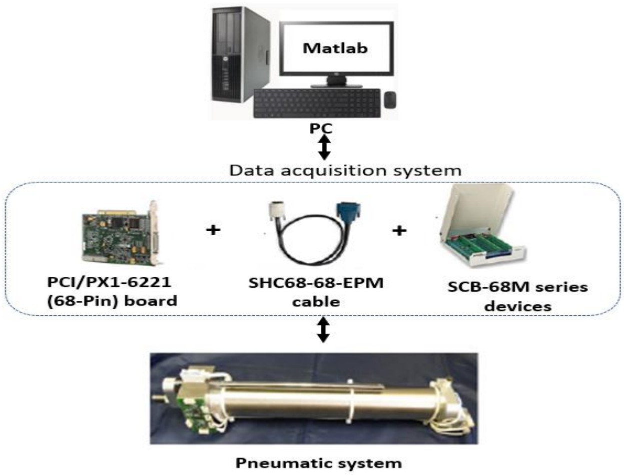


**Fig. 2 - The process of collecting input and output data**

For model identification, step input signal that injected into the valve was the input data while the position's signal was the output data. 2000 input and output data were collected at 0.01 sampling time. These data was then divided into two sets, where the first 1200 data was selected for estimation purposes while the next 800 data used for validation purposes. Equation (1) represents the transfer function identified with 91.84% fit with the actual plant and at minimum error value.

$$G(s) = \frac{0.3149\, s^2 + 3.325s + 0.6925}{s^3 + 5.793\, s^2 + 2.241\, s + 0.2154} \tag{1}$$

## 2.2 Development of the Controller

The development of the controller starts with the brief explanation of the PI controller, continued by an adaptive interaction theory, and the nonlinear AIA PI controller.

### 2.2.1 PI Controller

Equation (2) is a general mathematical expression of the PI controller. Here, *e(t)* is the deviation between the measured response to the referred response, while $K_p$ and $K_i$ are the proportional and integral gains of the controller, respectively. For a PI controller, the proportional (P), and integral (I) control actions are based on the error signal, *e(t)*, therefore the produced signals are summed to result the control signal, *u(t)* that is applied to the controlled plant.

$$u(t) = K_p\ e(t) + K_i\ \int_0^t e(t)dt \tag{2}$$

Even though the wide application of the PI controller in industrial sector is undeniable, but it still challenges of the PI to effectively deal with a complex nonlinear system due to the fixed $K_p$ and $K_i$. This motivates the modification of the conventional PI with adaptive interaction algorithm (AIA) that adaptively tune the PI control gains.

### 2.2.2 Adaptive Interaction Theory

According to the adaptive interaction's principle discussed in [16-17], a complex system can be divided into $N$ subsystems where each subsystem $n \in N := \{1,2,\dots N\}$ has integrable input and output signals. For each subsystem, the dynamic mapping of the input signal, $x_n$ to the output signal, $y_n$ can be defined by a causal functional as

$$F_n : x_n \rightarrow y_n, \quad n \in N \tag{3}$$

It means that, for the $n^{th}$ device, the output, $y_n(t)$ will relate to its input, $x_n(t)$ by

$$y_n(t) = (F_n \circ x_n)(t) = F_n[x_n(t)] \quad n \in N \tag{4}$$

where $o$ is the functional composition. To apply this algorithm, a Frechet derivative is assumed to exist, and each subsystem is considered as a single-input single-output (SISO) system.

Further, the interaction between two subsystems contains functional dependence of the input of one subsystem to the output of another subsystem. Let the connection carrying information is labelled as $c$ and the set of all connections as $C$. $pre_c$ is the subsystem whose output is conveyed by the connection $c$ while $post_c$ is the subsystem whose input depends on the information conveyed by the connection $c$. Therefore, the set of input for the $n^{th}$ subsystems can be defined as $I_n=\{c: pre_c = n\}$ while the output connections for the $n^{th}$ subsystems can be described as $O_n=\{c: post_c = n\}$. Example division or decomposition of a simple system based on adaptive interaction is shown in Figure 3. For this system, the set of input connections of Subsystem 2 can be defined as $I_2=\{c_1, c_3\}$ while the set of output connections is $O_2=\{c_4\}$. Also, $c_1$ connects Subsystem 1 and Subsystem 2, therefore $pre_{c1}$ = 1; $post_{c1}$ = 2. Detail on the adaptive algorithm theorem can be further referred in [16,17].

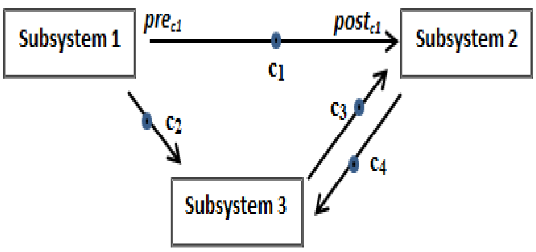


**Fig.3 - Interaction between subsystems**

It is noted that the input to a subsystem is a linear combination of the output of the other subsystems and summation of an external input signal, $u_n(t)$ as in Eq. (5) where the connection weights is labelled as $\alpha_c$.

$$x_n(t) = u_n(t) + \sum_{c \in I_n} \alpha_c y_{pre_c}(t), \qquad n \in N \tag{5}$$

The dynamic response, $y_n(t)$ is then expressed by

$$y_n(t) = F_n[u_n(t) + \sum_{c \in I_n} \alpha_c y_{pre_c}(t)], \quad n \in N \tag{6}$$

$F_n$ is indicated by Frechet derivative, thus result $\alpha_c$ as in Eq. (7). The adaptive interaction algorithm is targeted to adapt the $\alpha_{c;}$ therefore, the performance index, $E$ is minimized. If the $\alpha_c$ is adapted according to Eq. (6) then Eq. (5) performs a unique solution, and the performance index, $E$ decreases monotonically with time.

$$\dot{\alpha}_c = \left( \sum_{s \in 0post_c} \alpha_s \dot{\alpha}_s \frac{\frac{dE}{dy_{post_s}} \circ \dot{F}_{post_s}[x_{post_s}]}{\frac{dE}{dy_{post_s}} \circ \dot{F}_{post_s}[x_{post_s}] \circ y_{post_c}} - \gamma \frac{\partial E}{\partial y_{post_c}} \right) \circ \dot{F}_{post_c}[x_{post_c}] \circ y_{pre_c}, \; c \in C \tag{7}$$

$\Upsilon$ is the adaptive coefficient where $\Upsilon > 0$ then Eq. (9) can be further stated as Eq. (10).

$$\dot{\alpha}_c = -\gamma \frac{dE}{d\alpha_c}, \quad c \in C \tag{8}$$

$$\dot{\alpha}_c = -\gamma \frac{dE}{dy_{post_c}} \circ \dot{F}_{post_c}[x_{post_c}] \circ y_{pre_c} \tag{9}$$

As a result, an adaptive connection weight for PI controller can be referred as

$$\alpha_c := \{K_p, K_i\} \tag{10}$$

### 2.2.3 Nonlinear Adaptive PI Controller

The development of the conventional PI controller is extended to adaptive PI with an adaptive interaction algorithm (AIA). Figure 4 shows the construction of the adaptive PI where the *Kp* and *Ki* are now adaptively tuned by the AIA with respect to Eq. (10).

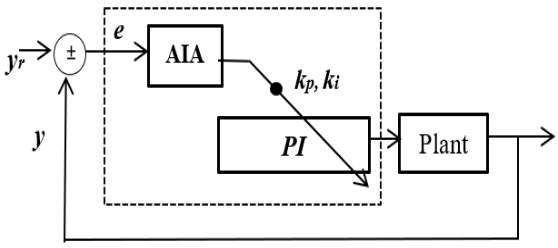


**Fig. 4 - The adaptive AIA PI**

According to Figure 4, the square of the error function, *E* can be described as

$$E = e^2 = (y - y_r)^2 \tag{11}$$

To minimize the error function, a gradient method is applied to $K_p$ and $K_i$ as

$$\begin{aligned} \dot{K}_p &= -\gamma \frac{dE}{dy} \circ \dot{F}[x] \circ y_p \\ \dot{K}_i &= -\gamma \frac{dE}{dy} \circ \dot{F}[x] \circ y_i \end{aligned} \tag{12}$$

As refers to [16,17], $\Upsilon$ is the adaptive coefficient while $\dot{F}$ is the Frechet derivative with respect to the plant input, *x* and the output, *y*. The adaptation algorithm in Eq. (12) is then reducing to

$$\begin{aligned} \dot{K}_p &= 2\gamma(y - y_r)^\circ \dot{F}[x]^\circ y_p \\ &= 2\gamma e^\circ \dot{F}[x]^\circ y_p \\ \dot{K}_\iota &= 2\gamma(y - y_r)^\circ \dot{F}[x]^\circ y_i \\ &= 2\gamma e^\circ \dot{F}[x]^\circ y_i \end{aligned} \tag{13}$$

According to (13), the tuning parameters, $K_p$ and $K_i$ are obviously dependent to the error, *e*, the Frechet derivative $\dot{F}[x]$ and the output of the proportional and integral parts, $y_p$ and $y_i$, respectively. The $\dot{F}[x]$ can be stated as

$$\dot{F}[x] \circ y = \int_0^t f_x(x(\tau), \tau)\ y(\tau) d\tau \tag{14}$$

where $f_x = \frac{\partial f}{\partial x}$.

Based on the convolution principle, the functional of *F[x]* can be described as

$$F[x] = g(t) * x(t) = \int_0^t g(t-\tau)\ x(\tau)d\tau \tag{15}$$

where * denotes the convolution while *g(t)* is the impulse response of the linear time-invariant system. Therefore, the Frechet derivative stated in (14) can be expressed as

$$\dot{F}[x] \circ y = g(t) * y(t) = \int_0^t g(t-\tau)\ y(\tau)d\tau \tag{16}$$

However, based on the previous study, the Frechet derivative in Eq. (16) can be approximated as Eq. (17) that applied in many practical systems such discussed in [18-20]. Here, $\sigma$ is a constant value while $y$ is an arbitrary function.

$$\dot{F}[x] \circ y = \sigma y \tag{17}$$

Therefore, the Frechet tuning algorithm can now be simplified as

$$\begin{aligned} \dot{K_p} &= 2\gamma e\dot{F}[x]^\circ y_p = 2\gamma e\sigma y_p \\ \dot{K_\iota} &= 2\gamma e\dot{F}[x]^\circ y_i = 2\gamma e\sigma y_i \end{aligned} \tag{18}$$

Let the $2\Upsilon\sigma = \eta$ and $\eta > 0$, the tuning algorithm can be simplified to numerical solutions as Eq. (19). This gives the adaptive controller parameters updated at every time, $t$ and applied in the development of the adaptive AIA PI controller.

$$\begin{aligned} \dot{K}p &= \eta e y_p \\ \dot{K}\iota &= \eta e y_i \end{aligned} \tag{19}$$

Nevertheless, from Eq. (19), the adaptive AIA PI has $\eta$ value to be initially tuned in the simulation. Difficulties come to identify the best value of $\eta$ especially when deals with complex nonlinear systems. This leads to the new modification of the adaptive AIA PI to be integrated with a nonlinear gain function as discussed in [22], hence developing the nonlinear adaptive AIA PI controller. Figure 5 shows the block diagram of the proposed nonlinear adaptive AIA PI which is the extension of Figure 4.

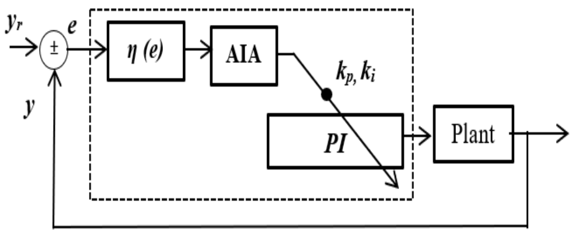


**Fig. 5 - The nonlinear adaptive AIA PI**

The nonlinear gain function applied is expressed as

$$\eta\ (e) = \frac{exp^{(k_n\ e)} + exp^{(-k_n\ e)}}{2}$$

Where

$$e = \begin{cases} e & |e| \leq e_{max} \\ sign(e) \cdot \sqrt{|e_{max}|} & else \end{cases} \tag{20}$$

Here, $e_{max}$ is a positive constant, $\eta$ is a functional of error based on the $k_n$ under the limitation of $0 \leq \eta(e) \leq \eta(e_{max})$. When $e$=0, the $\eta(e)$ is in the lower bounded gain, but when $e$=$e_{max}$, the $\eta(e)$ is in the upper-bounded gain. It is shown that the $e_{max}$ represents the range of variation while the $k_n$ indicates the rate of variation of $\eta(e)$.

With the nonlinear gain function, a good $\eta$ parameter is achieved, hence solving the tuning process of the AIA parameter. The resulted of the AIA parameter is next performs the best tuning of the *Kp* and *Ki* of the PI control gains. Therefore, improved transient response of the pneumatic positioning actuator will be resulted.

## 3. Result and Discussion

The aim of this study is to design a simple but effective controller that potentially improves the accuracy of the pneumatic actuator's cylinder stroke while maintaining its position at the desired level. Therefore, the proposed controller is expected to achieve improved steady-state error, $E_{ss}$ and settling time, $T_s$, with minimum percentage overshoots (%OS) of the system response.

The simulation starts with the development of a conventional PI controller. The trial-error method is used to find the PI controller gains, $K_P$ and $K_i$. Here, the $K_P$ and $K_i$ are set to 27 and 3.5, respectively. By maintaining the $K_p$ and $K_i$ as initial gain values in all operations, the development of the PI is extended to adaptive PI with adaptive interaction algorithm (AIA) to adaptively tune the *Kp* and *Ki*. As discussed previously, the adaptive AIA PI has $\eta$ value to be set in the simulation. Therefore, the $\eta$ is fixed to 0.001, 0.01, 0.1, and 1 while the response in tracking 100mm actuator's position are recorded. Next, a nonlinear gain function expressed in Eq. (20) is integrated into adaptive AIA PI that efficiently solves the tuning purposes of the $\eta$ value of the adaptive AIA PI controller.

The comparative output response of the actuator in retaining its position with conventional PID and PI controllers, with the adaptive AIA PI with fix tuning $\eta$ values continued by the response measured by the nonlinear adaptive AIA PI; labelled as nonL AIA is presented in Figure 6. Meanwhile, the steady-state error resulted is presented in Figure 7. The comparative transient responses of the controllers are explained in Table 1.

From Table 1, it was demonstrated that the integration of the AIA to conventional PI obviously minimize the steady-state error, *Ess*, improve the settling time, *Ts*, and reduce the overshoot, *OS*. Secondly, the difference $\eta$ of the AIA PI contributes to the impact of the output performances; therefore, ask for adaptive tuning for the best $\eta$ value. Third, a nonlinear gain function introduced to the AIA PI controller successfully yielded a good output response, compared to fixed AIA PI and obviosuy superior than conventional PI and PID controllers. The major improvement recorded by the overshoot, as presented in Table 2 where up to 4.22% overshoot was successfully reduced by the nonlinear adaptive AIA PI compared to AIA PI with $\eta$ =0.001. Besides, even though a close output responses were resulted compared to $\eta$=1, but the nonlinear adaptive AIA PI offers easy implementation due to automatic tuning of the $\eta$ value.

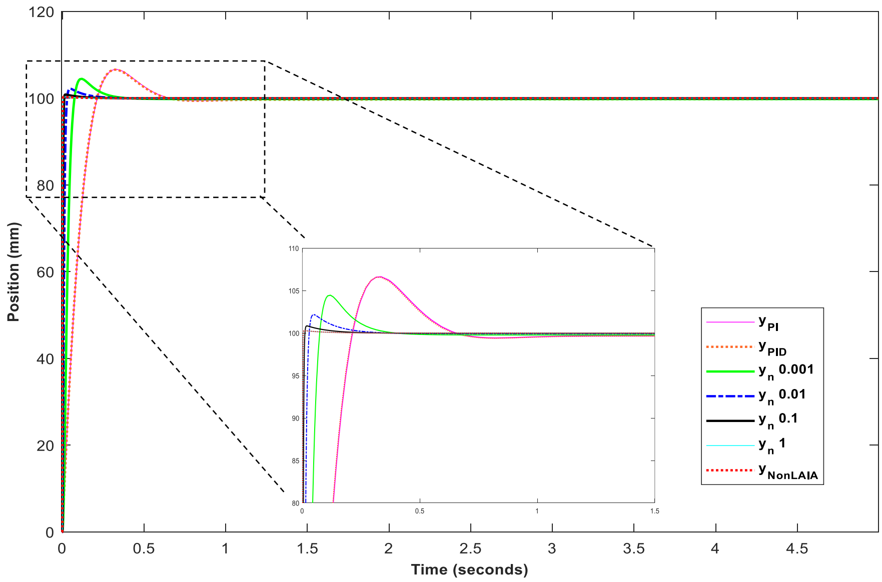


**Fig. 6 - The output control**

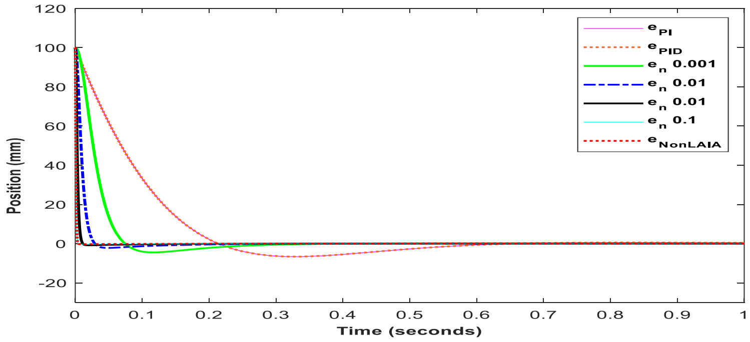


**Fig. 7 - The steady-state error**

**Table 1 - Comparative transient responses**

| Controller | Steady-state error, $E_{ss}$ | Settling time, Ts (s) | Overshoot, OS (%) |
|---|---|---|---|
| **PID** | 0.0454 | 0.65 | 6.5 |
| **PI** | 0.0459 | 0.65 | 6.6 |
| **AIA PI, $\eta$ =0.001** | 0.2038 | 0.34 | 4.5 |
| **AIA PI, $\eta$ =0.01** | 0.0648 | 0.19 | 2.2 |
| **AIA PI, $\eta$ =0.1** | 0.0205 | 0.05 | 0.8 |
| **AIA PI, $\eta$ =1.0** | 0.00648 | 0.015 | 0.29 |
| **NonL AIA PI** | 0.00647 | 0.015 | 0.28 |

**Table 2 - Deviation of percentage overshoot compared to NonL AIA PI**

| Controller | Deviation of OS (%) |
|---|---|
| **PID** | 6.22 |
| **PI** | 6.32 |
| **AIA PI, $\eta$ =0.001** | 4.22 |
| **AIA PI, $\eta$ =0.01** | 1.92 |
| **AIA PI, $\eta$ =0.1** | 0.52 |
| **AIA PI, $\eta$ =1.0** | 0.01 |

Figure 8 indicates the error performance indexes of the *Ess*, the integral absolute error (IAE), and integral time absolute error (ITAE) recorded by the controllers. The $\eta$ was again fixed to 0.001, 0.01, 0.1, and 1 while the response in tracking the 100mm actuators were recorded. It was evident that the error performance criterions are improved by the nonlinear adaptive AIA PI compared to fixed $\eta$ values in AIA PI and obviously compared to the conventional PID and PI controllers. Good tracking performance was demonstrated; hence accurate position of actuator's cylinder stroke was resulted that aimed in this study.

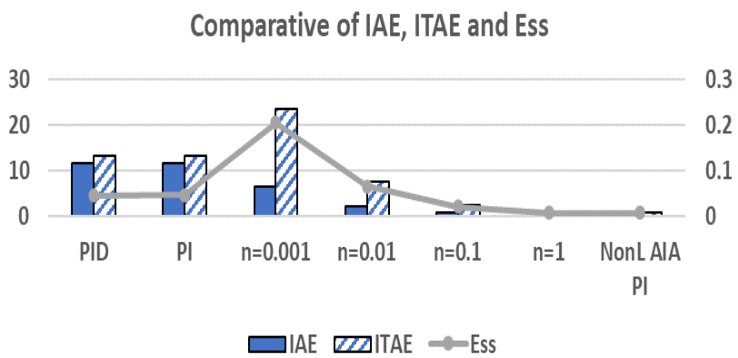


**Fig. 8 - Comparative of the error performance indexes**

To investigate the effectiveness of the nonlinear adaptive AIA PI controller, the particle swarm optimization (PSO) technique is applied to optimal tuning the $\eta$ value of the AIA PI parameter; labelled as PSO AIA and to optimal tuning the *Kp* and *Ki* of the PID, and PI controllers; labelled as PSO PID, and PSI PI. Again, the nonlinear adaptive AIA PI is labelled as NonL AIA. It was demonstrated that improved settling time, steady-state error and overshoots were resulted by the NonL AIA PI. These prove a good potential of the nonlinear adaptive AIA PI in tracking the actuator's position.

**Table 3 - The comparative performances with optimal PSO**

| | Settling time, Ts (s) | Overshoot, OS (%) | Steady-state error, $E_{ss}$ |
|---|---|---|---|
| **NonL AIA** | 0.015 | 0.28 | 0.00647 |
| **PSO AIA** | 0.3 | 0.5 | 0.01433 |
| **PSO PID** | 1.5 | 12 | 0.000151 |
| **PSO PI** | 1.0 | 20 | 0.00023 |

## 4. Conclusion

This study develops a nonlinear adaptive AIA PI controller based on an adaptive interaction algorithm (AIA). It can be summarized that the proposed controller successfully minimize the steady-state error, improved the settling time and reduce the overshoot of the pneumatic positioning response compared to the fixed adaptive AIA PI controller, and superiorly good than conventional PID and PI controllers. A good of the integral absolute error (IAE), and integral time absolute error (ITAE) recorded supported the effectiveness of the nonlinear adaptive AIA PI. Besides, the nonlinear adaptive AIA PI reduces the overshoot in the range of 0.22% to 19.72% compared to optimal PSO PID, PSO PI, and PSO AIA. The impact of the nonlinear adaptive AIA PI in obtaining the accurate position of the actuator's cylinder stroke was clearly proved besides effectively solving the tuning $\eta$ difficulties of the adaptive AIA PI controller.

## Acknowledgement

The authors would like to thank Universiti Teknikal Malaysia Melaka (UTeM) for their support. This support is gratefully acknowledged.

## References

[1] Jamian, S., Salim, S. N. S., Kamarudin, M. N., Zainon, M., Syed Mohamad, M. S., Abdullah, L., & Hanafiah, M. A. M. (2020). Review on controller design in pneumatic actuator drive system. TELKOMNIKA Telecommunication, Computing, Electronics and Control, 18(1), 332-342.

[2] Azahar, M. I. P., Irawan, A., Taufika, R. M., Suid, & M. H. (2020). Position Control of Pneumatic Actuator using Cascade Fuzzy Self-adaptive PID, 5th International Conference on Electrical, Control and Computer Engineering 2019. Lecture Notes in Electrical Engineering, 632.

[3] Osman, K., Ahmad Sukri, A. N., Sulaiman, S. F., Azira, A. R. & Faujan, M. F. (2019). Predictive Controller with Kalman Filter for Intelligent Pneumatic Actuator (IPA). Journal of Advanced Manufacturing Technology, 13, 2(2).

[4] Sulaiman, S. F., Rahmat, M. F., Faudzi, A. A. M., Osman, K., Syed Salim, S. N., Samsudin, S. I. & Azira, A. R. (2017). Enhanced Position Control for Pneumatic System by Applying Constraints in MPC Algorithm. International Journal of Electrical and Computer Engineering, 7(3).

[5] Osman, K., Mohd Faudzi, A. A., Rahmat, M. F., Mustafa, N. D., Suzumori, K. (2013). Predictive Functional Controller Design for Pneumatic Actuator with Stiffness Characteristic, IEEE/SICE International Symposium on System Integration (SII).

[6] Osman, K., Mohd Faudzi, A. A., Rahmat, M. F. & Sozumori, K. (2014). System Identification and Embedded Controller Design for Pneumatic Actuator with Stiffness Characteristic. Mathematical Problems in Engineering,13.

[7] Ormandzhiev, K., Yordanov, S. (2020). Design of Adaptive Fuzzy PID Controller for Electropneumatic System, E3S Web of Conferences.

[8] Ak-Dhaifallah, M., Kanagaraj, N., & Nisar, S. (2018). Fuzzy Fractional-Order PID Controller for Fractional Model of Pneumatic Pressure System. Mathematical Problem in Engineering, 5478781.

[9] Salim, S. N. S., Rahmat, M. F., Mohd Faudzi, A. A., Ismail, Z. H. & Sunar, N. H. (2014). Robust Control Strategy for Pneumatic Drive System via Enhanced Nonlinear PID Control. International Journal of Electrical and Computer Engineering, 4(5), 658-667.

[10] Sunar, N. H., Rahmat, M. F., Ismail, Z. H., Faudzi, A. A. M., Syed Salim, S. N., Samsudin, S. I. (2013). Application of optimization technique for PID tuning in position tracking of pneumatic actuator system, 2013 IEEE 9th International Colloqium on Sinal Processing and Its Application.
[11] Mohd Faudzi, A. A., Suzumori, K. & Wakimoto, S. (2010). Development of an Intelligent Chair Tool System Applying New Intelligent Pneumatic Actuators. Advanced Robotics, 24(10), 1503–1528.
[12] Mohd Faudzi, A. A., Suzumori, K., Wakimoto, S. (2010). Development of Pneumatic Actuated Seating System to Aid Chair Design, IEEE/ASME International Conference on Advanced Intelligent Mechatronics.
[13] Mohd Faudzi, A. A., Osman, K., Rahmat, M. F., Mustafa, N. D., Azman, M.A., & Suzumori, K. (2012). Controller Design for Simulation Control of Intelligent Pneumatic Actuators (IPA) System. Procedia Engineering, 41, 593–599.
[14] Mohd Faudzi, A. A., Osman, K., Rahmat, M. F., Suzumori, K., Din, N., & Azman, M. A. (2013). Real-time Position Control of Intelligent Pneumatic Actuator (IPA) System Using Optical Encoder and Pressure Sensor," Sensor Review, 33(4), 341–351.
[15] Sulaiman, S. F., Rahmat, M. F., Faudzi, A. A. M., & Osman., K. (2019). A new technique to reduce overshoot in pneumatic positioning system. TELKOMNIKA, 7(5), 2607-2616.
[16] Brandt, R. D. & F. Lin. (1999). Adaptive interaction and its application to neural networks. Information Sciences, 121:201 215.
[17] Badreddine, B. M., Zaremba, A., Sun, J. & Lin, F. (2001). Active Damping of Engine Idle Speed Oscillation by Applying Adaptive PID Control.The British Library.
[18] Shuai, A., Suozhong, Y., Huadong, L. (2016). Self-tuning of PID Controllers Design by Adaptive Interaction for Quadrotor UAV, Proceedings of 2016 IEEE Chinese Guidance, Navigation and Control Conference.
[19] Mahmud, Md., Motakabber, S. M. A., Zahirul Alam, A. H. M., Nordin, A. N. (2020). Adaptive PID Controller Using for Speed Control of the BLDC Motor, 2020 IEEE International Conference on Semiconductor Electronics.
[20] Rahmat, M. F., Samsudin, S. I., Abdul Wahab, N., Che Razali, M. & Gaya, M. S. (2013). Decentralized Adaptive PI with Adaptive Interaction Algorithm of Wastewater Treatment Plant. Jurnal Teknologi, 67(5).
[21] Adaptive PID Control Method and System for Internal Combustion Engine Rotation Speed Pulsation Damping. (2003). Patent No. US 6,591,808 B2.
[22] Su, Y. X., Sun, D. & Duan, B. Y. (2005). Design of an enhanced nonlinear PID controller. Mechatronics, 15, 1005-1024.